

Splattering During Turbulent Liquid Jet Impingement on Solid Targets

Sourav K. Bhunia

John H. Lienhard V

W. M. Rohsenow Heat and Mass Transfer Laboratory,
Department of Mechanical Engineering,
Massachusetts Institute of Technology,
Cambridge, MA 02139

In turbulent liquid jet impingement, a spray of droplets often breaks off of the liquid layer formed on the target. This splattering of liquid alters the efficiencies of jet impingement heat transfer processes and chemical containment safety devices, and leads to problems of aerosol formation in jet impingement cleaning processes. In this paper, we present a more complete study of splattering and improved correlations that extend and supersede our previous reports on this topic. We report experimental results on the amount of splattering for jets of water, isopropanol-water solutions, and soap-water mixtures. Jets were produced by straight tube nozzles of diameter 0.8–5.8 mm, with fully developed turbulent pipe-flow upstream of the nozzle exit. These experiments cover Weber numbers between 130–31,000, Reynolds numbers between 2700–98,000, and nozzle-to-target separations of $0.2 \leq l/d \leq 125$. Splattering of up to 75 percent of the incoming jet liquid is observed. The results show that only the Weber number and l/d affect the fraction of jet liquid splattered. The presence of surfactants does not alter the splattering. A new correlation for the onset condition for splattering is given. In addition, we establish the range of applicability of the model of Lienhard et al. (1992) and we provide a more accurate set of coefficients for their correlation.

1 Introduction

Liquid jets which impinge on solid surfaces often splatter violently, expelling a shower of droplets from the liquid film formed on the target. These airborne droplets are indicative of lowered cooling efficiency, lessened cleaning ability, or reduced coating efficiency, depending on the specific application of the impinging jet. In cleanroom situations, where impinging jets are used for post-etching debris removal, splattered liquid can produce airborne contaminants. In metal-jet forming operations, splattering is a primary cause of reduced yield. In situations involving toxic chemicals, the splattered droplets create a hazardous aerosol whose containment may necessitate significant air filtration costs.

Previous studies of splattering have demonstrated that it is driven by the disturbances on the surface of the impinging jet (Errico, 1986; Lienhard et al., 1992). Thus, undisturbed laminar jets do not splatter, unless they are long enough to have developed significant disturbances from capillary instability. Turbulent jets, on the other hand, develop surface roughness as a result of liquid-side pressure fluctuations driven by the turbulence, and they are highly susceptible to splattering.

Errico (1986) induced splattering of laminar jets by creating surface disturbances with a fluctuating electric field. His results showed that splattering commenced at progressively lower jet velocities when the amplitude of disturbance was increased. He also showed that splattering appeared on the liquid film

on the target as the disturbances from the jet spread radially. When a turbulent jet strikes a target, similar travelling waves originate near the impingement point and travel outward on the liquid film (see Fig. 1). When the jet disturbances are sufficiently large, these waves sharpen and break into droplets (Fig. 2). All observations indicate that the amplitude of these disturbances on the jet govern splattering. They further indicate that splattering is a non-linear instability phenomenon, since the liquid film is clearly stable to small disturbances but unstable to large ones (Varela and Lienhard, 1991).

Lienhard et al. (1992; called LLG hereinafter) reported measurements of the splattered liquid flow rate for turbulent

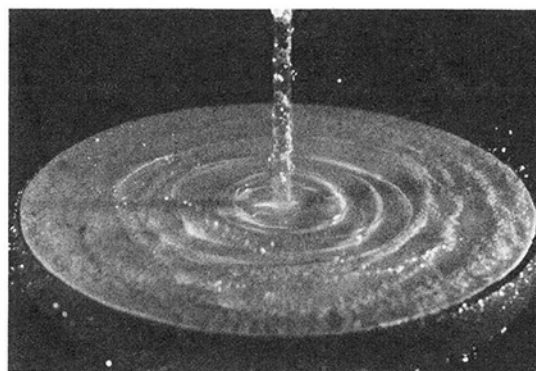


Fig. 1 Waves on the liquid layer and splattering. Water jet with $We_d = 2475$, $l/d = 31$, and $\xi = 0.108$ (Courtesy: X. Liu)

Contributed by the Fluids Engineering Division for publication in the JOURNAL OF FLUIDS ENGINEERING. Manuscript received by the Fluids Engineering Division October 27, 1992; revised manuscript received June 15, 1993. Associate Technical Editor: M. W. Reeks.

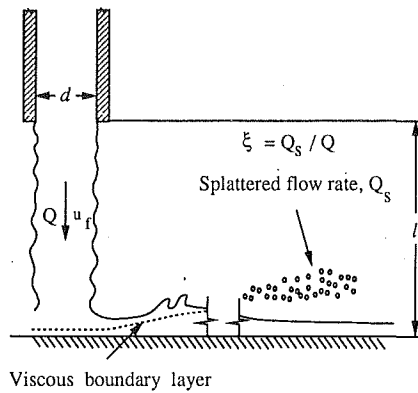


Fig. 2 Turbulent jet impingement and splattering: instantaneous liquid surface

jets in the form of the ratio of splattered flow rate, Q_s , to the incoming flow rate, Q :

$$\xi = \frac{Q_s}{Q} \quad (1)$$

LLG also proposed a model for splattering that related the rms amplitude of jet surface disturbances to the rate of splattering. In this model, turbulent pressure fluctuations in the jet formed an initial surface disturbance on the jet, which was then assumed to evolve by Rayleigh's capillary instability (Drazin and Reid, 1981) as the jet travelled to the target. The model produced a scaling parameter, ω , that characterized the rms amplitude of disturbances reaching the target:

$$\omega = We_d \exp\left(\frac{.971}{\sqrt{We_d}} \frac{l}{d}\right) \quad (2)$$

Here,

$$We_d = \rho u_f^2 d / \sigma \quad (3)$$

is the jet Weber number based on the average jet-velocity at the nozzle exit, u_f , the nozzle diameter¹, d , and the liquid surface tension, σ . The nozzle-to-target separation is l . LLG obtained good correlation between ξ and ω , leading to the result:

$$\xi = -0.0935 + 3.41 \times 10^{-5} \omega + 2.25 \times 10^{-9} \omega^2 \quad (4)$$

for $2120 \leq \omega \leq 8000$, with no splattering for $\omega < 2120$. LLG also noted that splattering occurred within a few diameters of the point of impact and that viscosity (in the form of a jet Reynolds

number) appeared to have no role in the splattering process, presumably owing to the thinness of the wall boundary layer in the stagnation region.

In spite of the LLG model's apparent success, several ambiguities accompany it. The model is based on data covering $1.2 \leq l/d \leq 28.7$ and $1000 \leq We_d \leq 5000$, and its validity outside that range is unestablished. The onset point for splattering shows significant scatter as a function of ω and is not in complete agreement with all observations by other investigators. Furthermore, the model is predicated on exponential growth of capillary disturbances at the rate corresponding to Rayleigh analysis' most unstable wavelength ($\lambda = 4.51d$). That assumption is obviously flawed, since the turbulent pressure fluctuations driving instability cover a broad range of much shorter wavelengths ($\lambda < d$), the most energetic of which should be stable according to Rayleigh's results.

The present paper examines splattering over a much broader range of Weber number and nozzle-to-target separations ($130 < We_d < 31,000$; $0.2 < l/d < 125$). Surface tension is independently varied. In contrast to LLG, we treat We_d and l/d as independent parameters. Our objectives are to establish the range of applicability of the LLG model and to obtain a more generally applicable criterion for the onset of splattering beneath a turbulent impinging liquid jet. In addition, we attempt further explanation of the overall phenomenon of splattering in terms of the available data on the evolution of surface-disturbances on turbulent jets.

2 Experiments

A schematic diagram of the measurement system is given in Fig. 3. All the measurements were made with water jets issuing into still air. Tube nozzles having diameters between 0.8-5.8 mm were used to produce the jets. The tubes were made 70-100 diameters long so as to ensure fully developed turbulent flow at the tube outlet. The outlets were carefully deburred to prevent the introduction of mechanical surface disturbances. The tube nozzles received water from a pressurized plenum with disturbances dampers and honeycomb flow straighteners at its upstream inlet.

Nozzle-target separation was varied from 2 to 300 mm. This corresponds to nondimensional nozzle-target separations, l/d , between 0.2 and 125 for all the nozzles other than the 0.84 mm diameter nozzle, for which l/d reached 500.

Splattering takes place over a limited range of radial positions upstream of the hydraulic jump, typically within a few diameters of the point of impact. The target radius was between 2 and 50 cm, and always slightly larger than the radial location of the hydraulic jump. The amount of liquid that remained in the liquid sheet on the target after splattering was measured by collecting it in a container beneath the target. The splattered liquid, on the other hand, remained airborne and fell well beyond the rim of the container. Flow rates of the jet and of

¹The contraction coefficient for turbulent jets leaving pipe nozzles is nearly unity. Throughout this study, we treat nozzle diameter and jet diameter interchangeably.

Nomenclature

d = nozzle diameter (m)	Q_s = flow rate of splattered liquid (m^3/s)	λ = jet surface disturbance wavelength (m)
f = Darcy friction factor	u_f = average jet velocity at the nozzle exit (m/s)	μ = liquid dynamic viscosity ($kg/m \cdot s$)
l = nozzle-to-target separation (m)	u' = rms fluctuating component of velocity (m/s)	ξ = splattered fraction of incoming jet's liquid, Q_s/Q
l_b = jet breakup length (m)	u_* = friction velocity based on wall shear stress, $u_f \sqrt{f}/8$ (m/s)	ρ = liquid density (kg/m^3)
l_c = length of the jet at which splattering reaches its asymptotic limit (m)	x = distance along the jet axis from the nozzle exit (m)	σ = surface tension between liquid and the surrounding gas (N/m)
l_o = length of the jet corresponding to onset of splattering (5 percent threshold) (m)	δ = rms height of the jet surface disturbances (m)	ω = splattering parameter defined by Eq. (2)
Q = jet flow rate (m^3/s)		Re_d = jet Reynolds number, $\rho u_f d / \mu$
		We_d = jet Weber number, $\rho u_f^2 d / \sigma$

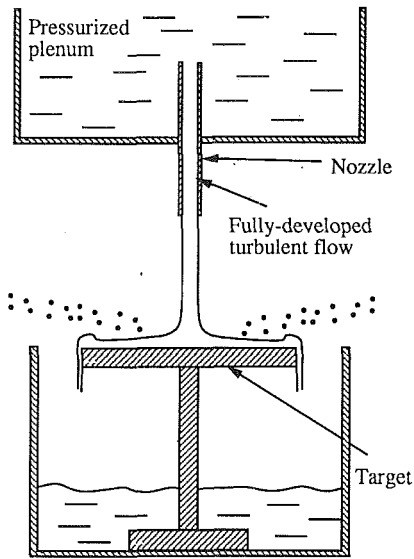


Fig. 3 Measurement of the fraction of jet liquid splattered

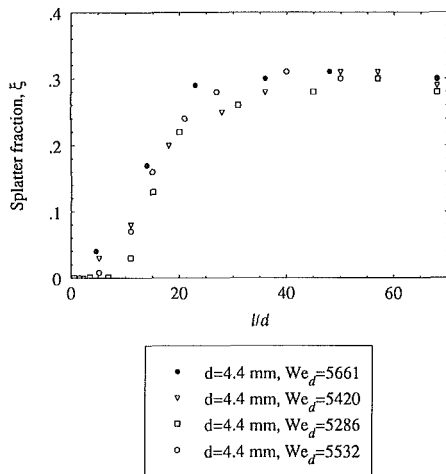
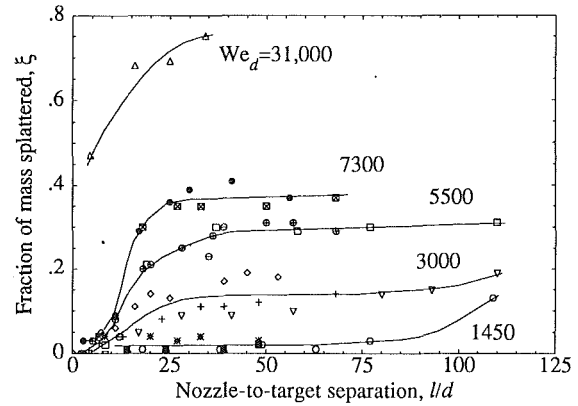


Fig. 4 Scatter in the measurements of splatter fraction for water jets of nearly the same Weber numbers

the unsplattered liquid were both obtained by measuring the time required to collect a known volume of liquid. From this, the amount of splattering was calculated.

The liquids used in these experiments were water, an isopropanol-water solution, and water containing a surfactant detergent. The liquid temperature was between 21 and 27°C. Surface tension was measured several times during the experiments using a platinum-ring surface tension meter. Tube diameters were measured and checked for roundness, and these measured values of diameter were used in all subsequent calculations.

This technique facilitated quite precise measurements of the amount of splattering. Typically the uncertainty in ξ (at 95 percent confidence) was below ± 5 percent for $\xi > 10$ percent and below ± 25 percent for $\xi < 4$ percent. Uncertainties in the Reynolds numbers and the Weber numbers were below ± 2 and ± 3 percent, respectively. These low uncertainties may be credited to the direct measurement of liquid flow rate. Uncertainties in l/d and ω were below ± 2 and ± 3 percent, respectively. Some of the measurements were repeated using two different pumps to verify the reproducibility of the data and their independence from upstream pressure fluctuations. Figure 4 shows the typical scatter in the measurements of splatter fraction for several different runs at nearly the same jet Weber



△	$d=4.4$ mm, $Re_d=98097$, $We_d=31243$
⊠	$d=4.4$ mm, $Re_d=48284$, $We_d=7564$
●	$d=2.7$ mm, $Re_d=37141$, $We_d=7096$
⊙	$d=5.8$ mm, $Re_d=47800$, $We_d=5628$
⊕	$d=4.4$ mm, $Re_d=41437$, $We_d=5420$
□	$d=2.7$ mm, $Re_d=31868$, $We_d=5373$
◇	$d=5.8$ mm, $Re_d=35986$, $We_d=3101$
+	$d=4.4$ mm, $Re_d=30090$, $We_d=2858$
▽	$d=2.7$ mm, $Re_d=24580$, $We_d=3108$
*	$d=5.8$ mm, $Re_d=24507$, $We_d=1479$
■	$d=4.4$ mm, $Re_d=20988$, $We_d=1430$
○	$d=2.7$ mm, $Re_d=16320$, $We_d=1409$

Fig. 5 Splattering as a function of nozzle-target separation and jet Weber number. Solid lines are fitted curves for Weber number constant to within ± 3 percent (which is the uncertainty of the experimental We_d): $We_d = 1450$ (1409, 1430, 1479); 3000 (3108, 2858, 3101); 5500 (5373, 5420, 5628); 7300 (7096, 7564); 31000 (31243).

numbers. (The values are all within the ± 3 percent uncertainty limits of We_d .) The rms scatter in ξ from run to run is ± 4 percent of the maximum value of ξ of about 0.3.

The independent physical parameters involved in this problem are l , d , ρ , u_j , σ , and μ . Dimensional analysis based on these parameters shows that the fraction of liquid splattered, ξ can depend only on three dimensionless groups, namely l/d , Re_d , and We_d . Independent variation of these three groups was accomplished by independent variation of d , l , σ , and u_j .

3 Splattering and Its Relation to Jet Disturbances

Figure 5 shows the amount of splattering at different nozzle-target separations for several nozzle diameters and Reynolds numbers. Each solid line represents data for a narrow range of Weber numbers, varying by less than ± 3 percent around the stated mean value, a range equal to the experimental uncertainty of We_d . Splattering of as much as 75 percent of the incoming fluid is observed at a Weber number of 31,000 and a Reynolds number of 98,000 for a nozzle-target separation of $l/d = 34$.

At any given Weber number and nozzle-target separation, the splatter fraction, ξ , depends extremely weakly on the Reynolds number, if at all. For example, in the data set for $We_d = 5500$, the Reynolds number increases by a factor of 1.5 without any discernible change in the splatter fraction, ξ . In contrast, a factor of 1.3 increase in the Weber number (from 5500 to 7300) produces a significant increase in the splatter fraction (roughly +25 percent).

An influence of Reynolds number would be expected to arise primarily from viscous effects near solid boundaries, either in setting the pipe turbulence intensity or as an influence of the viscous boundary layer along the target. Past work (e.g., Lien-

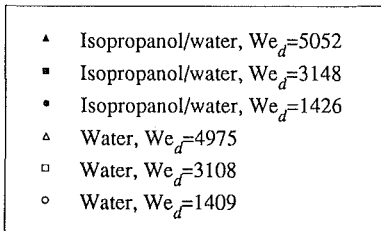
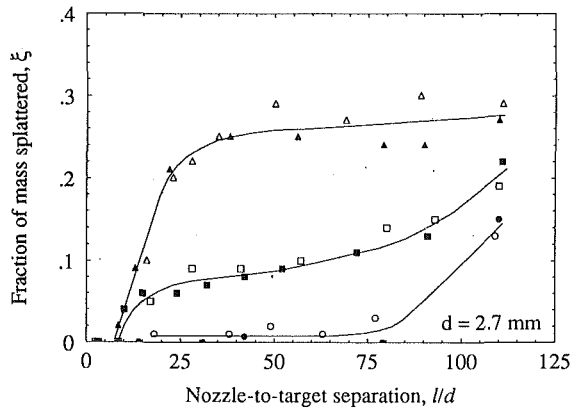


Fig. 6 (a) The Weber number correlates the splatter fraction, ξ , as the surface tension of the jet liquid is varied (0.072 N/m for water and 0.042 N/m for isopropanol/water solution): $d = 2.7$ mm

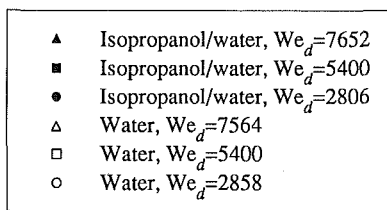
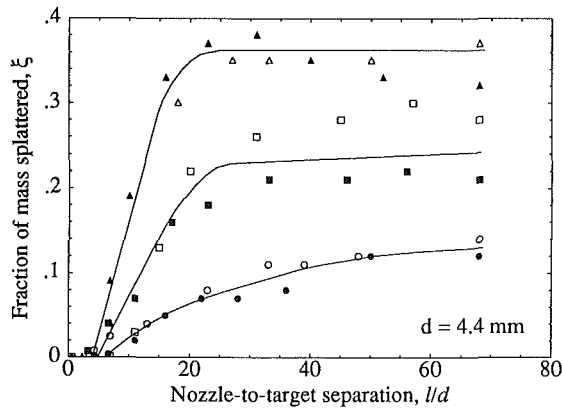


Fig. 6 (b) The Weber number correlates the splatter fraction, ξ , as the surface tension of the jet liquid is varied (0.072 N/m for water and 0.042 N/m for isopropanol/water solution): $d = 4.4$ mm

hard et al., 1992) has established that the stagnation-point boundary layer is extremely thin relative to the liquid layer, and it thus may have little effect on the surface waves near the stagnation-point. To examine the effect of Reynolds number on turbulence intensity we refer to Laufer (1954). His measurements show the ratio of rms turbulent speed to friction velocity, u'/u_* , to be nearly independent of Reynolds number in fully-developed turbulent pipe-flows. Therefore

$$\frac{u'}{u_f} \propto \frac{u_*}{u_f} \propto \sqrt{f} \propto Re_d^{-1/8}$$

where we have used the definition of $u_*(=u_f\sqrt{f/8})$ and the

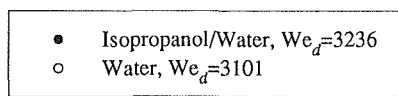
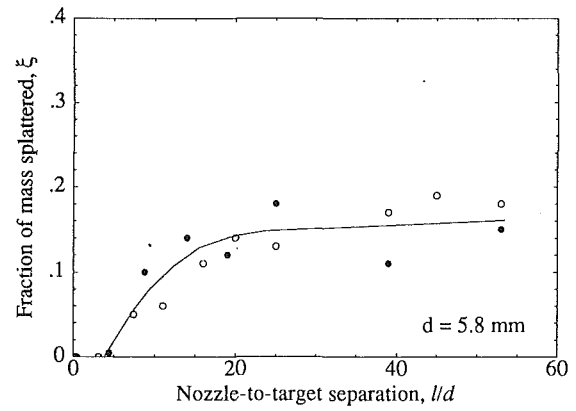


Fig. 6 (c) The Weber number correlates the splatter fraction, ξ , as the surface tension of the jet liquid is varied (0.072 N/m for water and 0.042 N/m for isopropanol/water solution): $d = 5.8$ mm

Blasius friction factor equation ($f = .316Re_d^{-1/4}$ for $4000 < Re_d < 10^5$). This weak dependence of the turbulence intensity on the Reynolds number may be the reason that we observe no significant dependence of splattering on the jet Reynolds numbers over the present range of Re_d .

To study the effect of surface tension variation on splattering, a solution of approximately 10 percent by volume of isopropanol in water was used. The surface tension of the solution was measured before each run of the experiment; it was thus maintained at 0.042 N/m within ± 5 percent accuracy (versus 0.072 N/m for pure water). Density was also measured. The data show (Figs. 6 a, b, c) that the splatter fraction, ξ , still scales with Weber number, We_d , as observed before for the water jets. The splatter fraction data for water and for an isopropanol-water solution, at a given jet Weber number, agree to within the experimental uncertainty in all but one case (Fig. 6b, $We_d = 5368$).

Referring to Figs. 5 and 6, we see that very little splattering occurs close to the jet exit (small l/d), typically less than 5 percent. Beyond this region, the amount of splattering at first increases with distance, l/d . Farther downstream, it reaches a plateau. To explain these observations we refer to some recent measurements of the amplitude of turbulent liquid jet surface disturbances (Bhunia and Lienhard, 1993). The rms amplitude of jet surface disturbances at different axial locations of the jet, were obtained from the measurements of the instantaneous disturbance amplitude, using a non-intrusive optical instrument. Starting from nearly zero near the nozzle exit, the rms amplitude of jet surface disturbances initially grows rapidly as the jet moves downstream; farther downstream the growth rate diminishes and the rms disturbance tends to an asymptotic limit. Earlier Chen and Davis (1964) attempted to measure the amplitude of surface disturbances on turbulent liquid jets by an electric conductivity probe. Although that method is less accurate owing to the interference of the probe with the flow, those measurements are qualitatively consistent with the optical data. This growth of disturbances is the probable cause of the increase in the splatter fraction as the jet moves downstream. The steadily decreasing rate of amplitude growth results in a plateau of the disturbance amplitude which corresponds to that in the splatter fraction data.

For very long, low Weber number jets the plateau of splattering ends and ξ again increases with l/d (Fig. 6a). This may reflect the appearance of ordinary capillary instability on these jets. Specifically, when the Weber is low, the asymptotic turbulence-generated surface roughness is small compared to the

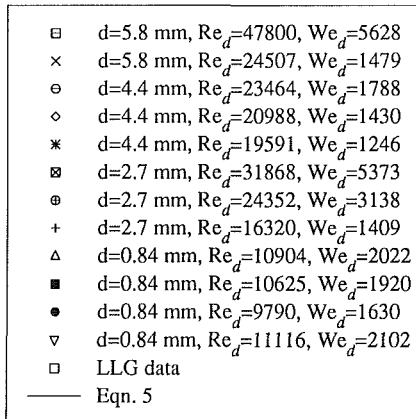
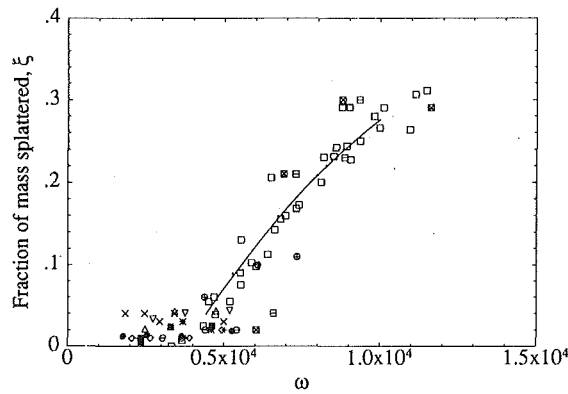


Fig. 7 Comparison of the LLG model's scaling with the present data for $l/d < 50$

jet radius. Thus, the still nearly-cylindrical jet can give up surface energy by the usual Rayleigh-type instability. In contrast, at higher Weber number the turbulent disturbances grow to be as large as the jet radius, effectively breaking up the jet. In the low Weber number case, the splattering plateau ends when capillary instability further raises the jet roughness. In the high Weber number case, the plateau is reached when the jet is essentially broken up into drops.

Once the jet is broken up, the splattering is effectively due to the impact of individual droplets. For a given Weber number, the size and velocity of those droplets remain nearly constant with increasing l/d (excluding the effect of air drag); thus the amount of splatter reaches an asymptotic value. Presumably, this asymptote depends on droplet Weber number (which is roughly equal to jet Weber number).

On the basis of the present experiments, we find that the range of applicability of the LLG model is $10^3 < We_d < 5 \times 10^3$, $l/d < 50$ and $4400 < \omega < 10,000$. Figure 7 shows both the present data and the LLG data in $\xi - \omega$ coordinates. The scaling with ω correlates the data reasonably well in this range. While LLG used nominal tube diameter in their data reductions, all data in Fig. 7 are scaled with measured diameter. On this basis, we offer the following improved correlation for $\xi(\omega)$ in the range $4400 < \omega < 10,000$:

$$\xi = -0.258 + 7.85 \times 10^{-5} \omega - 2.51 \times 10^{-9} \omega^2 \quad (5)$$

The lower limit in terms of ω is chosen to ensure that the predicted ξ is at least 4 percent. Below this level there is considerable scatter and high uncertainty in the measurements.

For larger l/d or We_d , the ω model fails (Fig. 8), but a different pattern emerges. For $We_d = \text{constant}$, ω becomes a function of l/d only and we see curves similar to the ones in Fig. 5.

3.1 The Influence of Surfactants. Surfactants lower liquid surface tension by forming a surface-absorbed monolayer

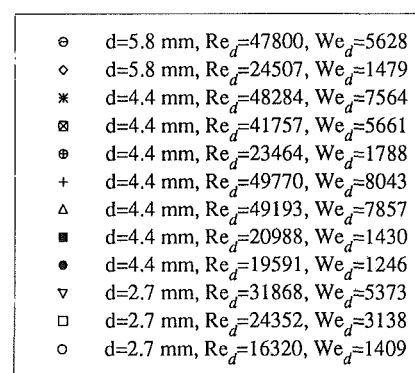
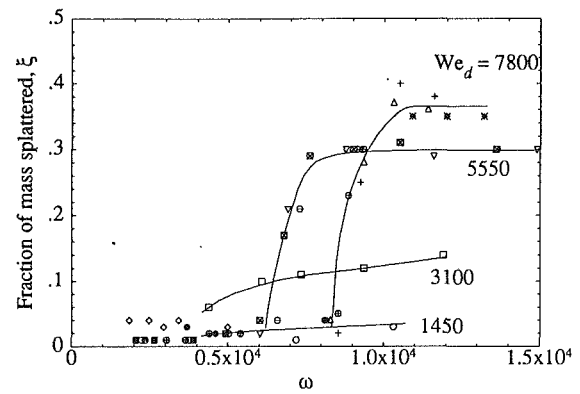


Fig. 8 Breakdown of the LLG model for $l/d > 50$ or $We_d > 5000$

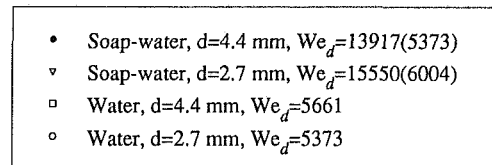
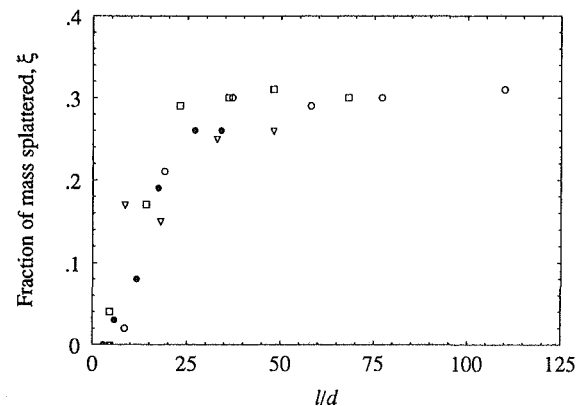


Fig. 9 Effect of surfactants on splattering. The Weber number in parentheses is based on the surface tension of pure water.

at the liquid surface. When a new liquid surface is formed, some time is required for surfactant molecules to diffuse to the surface in sufficient concentration to alter the surface tension. To study the role of surfactants in splattering, a mixture of approximately 0.2 percent detergent in water was used. This reduced the surface tension of the static solution (liquid surface at rest) to 0.027 N/m and corresponded to a saturated concentration of surfactant. Figure 9 shows that the presence of the surfactant does not alter the amount of splattering. The splatter friction for the surfactant-laden jet is identical to that for a pure water jet of the same velocity, diameter and length; in fact, if the surfactant-jet Weber number is calculated on

the basis of pure-water surface tension, the curves for the surfactant-jets are identical to those of the pure jets. From the standpoint of splattering, the surface tension of the surfactant-jet is effectively the surface tension of the pure liquid.

Possible reasons for this behavior are as follow. Inside the nozzle, the surfactant is in the bulk of the liquid. When the liquid exits the nozzle, a new free surface is formed which is not initially saturated with surfactant. Because a finite time is required for the surfactant to diffuse from the bulk to the free surface, the surface remains unsaturated over some initial length of the jet. In this initial region, the surface tension remains near that of pure water.

The time required for the surface concentration of surfactant to reach saturation was estimated for turbulent diffusion from the bulk to the free surface under the assumption that all surfactant reaching the surface is captured by and remains on the surface. Using Köhler's (1993) correlation for interphase mass transfer across free surface, this model yields an unsaturated length of only 3 to 4 diameters for the two cases in Fig. 9. However, the model is unreasonable in that it neglects any turbulent reentrainment of surfactant from the surface, to the bulk, an effect that is probably quite large. Thus it seems likely that the time required to achieve saturation is significantly longer, if saturation is reached at all. In consequence, only the surface tension of the bulk liquid appears to play a role in splattering, at least for the lengths of the jets in this study. The data show clearly that the presence of a surfactant does not alter the splattering characteristics.

To help resolve this issue, measurements of the jet surface-roughness evolution with surfactants could be compared to those without surfactant. The present data and the belief that the splattering is driven by surface disturbances together imply that a surfactant has no impact on roughness evolution. These measurements will be the subject of future work.

3.2 The Onset of Splattering. Some problems arise in defining the onset point of splattering. Since the process of splattering involves turbulent flow, sporadic splattering of droplets occurs at much lower jet velocities than those that would cause any significant amount of sustained splattering (other parameters remaining the same). Consequently, the onset point is more accurately definable in terms of a non-zero level of splattering. Owing to the finite accuracy of measurement systems, this threshold should not be so low as to have substantial uncertainty. We chose to define the onset of splattering as the point where 5 percent of the incoming fluid is splattered. In view of our earlier observation that, for a given l/d , the amount of splattering depends strongly on the jet Weber number and not on the Reynolds number, we expect the onset point to be uniquely identifiable by its l/d and We_d . In other words, for a jet of a given Weber number, the onset point is reached at a certain l/d .

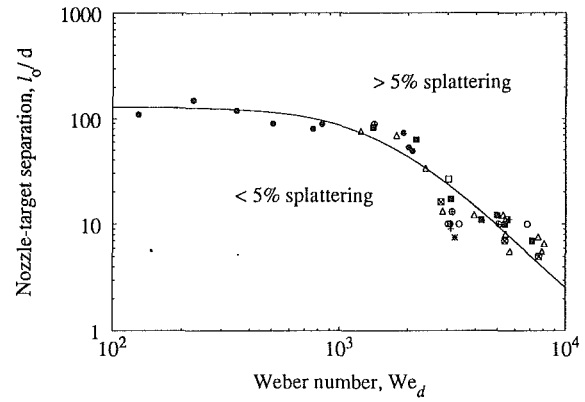
Figure 10 shows the data for onset points. A correlation for the onset point data is

$$\frac{l_o}{d} = \frac{130}{1 + 5 \times 10^{-7} We_d^2} \quad (6)$$

For low Weber numbers, where surface tension dominates, comparison to the capillary breakup length is appropriate. When aerodynamic forces are negligible, the capillary breakup length of a uniform-velocity jet is given by (Weber, 1931)

$$\frac{l_b}{d} = 12\sqrt{We_d} \left(1 + \frac{3\sqrt{We_d}}{Re_d} \right) \quad (7)$$

For the turbulent jets in this study, produced by fully-developed turbulent pipe-flows, Re_d exceeds 2000. In such jets, when $We_d \sim 100$ we find $l_b/d \sim 120$. Thus, the observed onset point at low Weber numbers is close to the capillary breakup point. In this range, splattering is essentially of drop impingement type. Apparently, turbulent disturbances are strongly damped



×	d = 5.8 mm, Isopropanol/water
⊠	d = 4.4 mm, Isopropanol/Water
⊙	d = 2.7 mm, Isopropanol/Water
+	d = 5.8 mm, Water
△	d = 4.4 mm, Water
⊠	d = 2.7 mm, Water
•	d = 0.84 mm, Water
—	Eqn. 6
□	Lienhard et al. (1992)
○	Womac et al.(1990)

Fig. 10 Onset of splattering

Table 1 Comparison of observed upper-limit lengths to predicted capillary/aerodynamic breakup lengths of Miesse (1955)

We_d	Re_d	l_c/d	l_b/d	l_b/l_c
5373	31868	25	61	2.44
5661	41757	24	53	2.2
7564	48284	20	56	2.8
8043	49770	18	56	3.1

by surface tension in these low Weber number jets, and capillary instability is dominant.

The relative importance of turbulence and surface tension is characterized by a balance of the rms turbulent dynamic pressure and the capillary pressure. Thus, the appropriate Weber number for characterizing the splattering mechanism is based on the rms fluctuating component of the velocity, u' , and the rms height of the surface disturbances, δ :

$$We' = \frac{\text{turbulent dynamic pressure}}{\text{capillary pressure}} = \frac{\rho u'^2}{\sigma/\delta} = \frac{\rho u'^2 \delta}{\sigma} \quad (8)$$

We' should be $\mathcal{O}(1)$ or greater when turbulence drives splattering. However, u' and δ are not easily available, while u_f and d are, so we have used

$$We_d = \frac{\rho u_f^2 d}{\sigma} = We' / \left[\frac{\delta}{d} \left(\frac{u'}{u_f} \right)^2 \right] \gg 1 \quad (9)$$

which is 100-1000 times larger than the Weber number, We' , that actually characterizes physical processes involved here (since u'/u_f is a few percent in magnitude and $\delta/d < 0.5$).

The only other quantitative data on onset in literature – LLG and Womac et al. (1990)—compare very well with the present study. Some data in the text and in an accompanying figure in the paper by Womac et al. were combined to obtain the onset points for their study. Apparently, they identified the onset points by visual observations. This is likely to provide slightly different l_o/d than by our method. Also, the visual determination of onset point depends on the size of the splattered droplets and their optical properties, which in turn in-

roduce additional uncertainties. These factors may account for the slight discrepancies between their results and ours.

Stevens and Webb (1989) did not observe any splattering for their turbulent jets (Webb, 1991). The most likely reason for this is that, in their study, l/d was almost always smaller than l_c/d . Only two of their reported data points lie within our splattering region (specifically, $Re_d = 5 \times 10^4$, $d = 5.8$ mm, $l/d = 12.8$, $We_d = 6.2 \times 10^3$ and $Re_d = 4 \times 10^4$, $d = 4.1$ mm, $l/d = 18.5$, $We_d = 5.6 \times 10^3$).

LLG reported an onset criterion of $\omega \geq 2120$ for the appearance of any splattering. In contrast, the present data show onset of any splattering over a range of values of ω , $2000 < \omega < 8000$. Within the range of applicability of the LLG model that was mentioned above, the onset of 5 percent splattering occurred for ω between 4100 and 5100.

3.3 The Upper Limit of Splattering for High Weber Number Jets. As previously explained, the upper limit of splattering for high Weber number jets should be reached near the breakup length of the jet. The breakup length of turbulent jets is known to depend on Reynolds and Weber numbers (Lienhard and Day, 1970). Miesse (1955) reported correlations for breakup lengths, l_b , of turbulent liquid jets subject to strong aerodynamic forces. From the data on jets from industrially-used converging-orifice type nozzles in a Reynolds number range similar to ours, he reported

$$\frac{l_b}{d} = 540 \sqrt{We_d} Re_d^{-5/8} \quad (10)$$

The jets in the present study were produced by tube nozzles with fully developed turbulent flow, so their breakup lengths can be predicted only in order of magnitude by this correlation. Table 1 compares the breakup lengths predicted by this correlation to the nozzle-target separations, l_c , at which the asymptotic upper limit of splattering is reached.

The predicted breakup lengths l_b are larger than the upper limit lengths l_c roughly by a factor of 2.6. This may be because this correlation overestimates the breakup lengths for the different nozzle geometry involved here. Alternatively, it may be that the splattering mechanism changes from jet impingement splattering to drop impingement splattering somewhat before the jet breakup location. In either case, the comparison shows a consistent relation between the jet breakup length and the upper-limit length of splattering.

4 Conclusions

Splattering has been measured for turbulent liquid jets impinging solid targets. Data span the range $0.2 \leq l/d \leq 125$, $2700 \leq Re_d \leq 98,000$ and $130 \leq We_d \leq 31,000$. The present results have been compared to the previous studies and improved correlations have been developed.

- For a turbulent jet, the amount of splattering is governed by the level of surface disturbances present on the surface of jet. This observation is similar to those for laminar jets with externally-imposed disturbances.

- The amount of splattering at a given nozzle-target separation depends principally on the jet Weber number.

- The presence of surfactants in the jet does not alter the amount of splattering. Only the surface tension of the bulk fluid plays a role in splattering.

- The model proposed by Lienhard et al. (1992) is applicable for $1000 < We_d < 5000$ and $l/d < 50$. An improved version of their correlation is $\xi = -0.258 + 7.85 \times 10^{-5} \omega - 2.51 \times 10^{-9} \omega^2$, for $4400 < \omega < 10,000$. Outside this range, We_d and l/d should be treated as independent parameters.

- The onset point of splattering for a 5 percent threshold is given by the correlation $l_c/d = 130/(1 + 5 \times 10^{-7} We_d^2)$.

- The upper-limit length of splattering, beyond which ξ is constant, appears to be related to the jet breakup length.

- Over the range of Reynolds numbers in this work, no significant effect of jet Reynolds number is identifiable. However, a very weak dependence on Reynolds number is likely to be present in all of the conclusions and the correlations presented in this study. Extrapolation above $Re_d = 100,000$ should be done skeptically.

Acknowledgments

We gratefully acknowledge the support of the National Science Foundation under grant number CBT 8858288.

References

- Bhunja, S. K., and Lienhard V, J. H., 1993, "Surface Disturbance Evolution and the Splattering of Turbulent Liquid Jets," *Heat Transfer—Atlanta, 1993*, AIChE Symposium Series, Vol. 89, No. 295, pp. 1–8.
- Chen, T.-F., and Davis, J. R., 1964, "Disintegration of a Turbulent Water Jet," *Journal of Hydraulics Division, Proceedings of ASCE*, HY 1, Jan. pp. 175–206.
- Drazin, P. G., and Reid, W. H., 1981, *Hydrodynamic Stability*, Cambridge University Press.
- Errico, M., 1986, "A Study of the Interaction of Liquid Jets with Solid Surfaces," Ph.D. thesis, University of California, San Diego.
- Köhler, J., 1993, "Heat and Mass Transfer in a Two-Phase Flow of a Binary Mixture," Heat Transfer Lab Internal Report, Department of Mechanical Engineering, MIT, Cambridge, MA.
- Laufer, J., 1954, "The Structures of Turbulence in Fully Developed Pipe Flow," NACA Technical Report No. 1174.
- Lienhard, J. H., and Day, J. B., 1970, "The Breakup of Superheated Liquid Jets," *ASME Journal of Basic Engineering*, pp. 515–522.
- Lienhard V, J. H., Liu, X., and Gabour, L. A., 1992, "Splattering and Heat Transfer During Impingement of a Turbulent Liquid Jet," *ASME Journal of Heat Transfer*, Vol. 114, May, pp. 362–372.
- Miesse, C. C., 1955, "Correlation of Experimental Data on the Disintegration of Liquid Jets," *Industrial and Engineering Chemistry*, Vol. 47, Sept., pp. 1690–1701.
- Stevens, J., and Webb, B. W., 1989, "Local Heat Transfer Coefficients Under an Axisymmetric, Single-Phase Liquid Jet," *Heat Transfer in Electronics-1989*, ASME HTD, Vol. 111, pp. 113–119 (National Heat Transfer Conference, Philadelphia, PA).
- Varela, D. A., and Lienhard V, J. H., 1991, "Development of Non-Linear Waves on a Non-uniform Axisymmetric Film," *Bulletin of American Physical Society*, A18, Vol. 36, No. 10; 44th Annual Meeting of Division on Fluid Dynamics, Scottsdale, AZ.
- Weber, C. 1931, "Zum Zerfall eines Flüssigkeitsstrahles," *Zeitschrift für angewandte Mathematik und Mechanik*, Vol. 2, pp. 136–154.
- Webb, B. W., 1991, personal communication, July.
- Womac, D. J., Aharoni, G., Ramadhyani, S., and Incropera, F. P., 1990, "Single Phase Liquid Jet Impingement Cooling of Small Heat Sources," *Proceedings 9th International Heat Transfer Conference*, Jerusalem, Israel, Vol. 4, pp. 149–154.